Viscous parallel flows in finite aspect ratio Hele-Shaw cell: Analytical and numerical results

Philippe Gondret, N. Rakotomalala, Marc Rabaud, D. Salin, P. Watzky

Viscous parallel flows in finite aspect ratio Hele-Shaw cell: Analytical and numerical results

P. Gondret, N. Rakotomalala, M. Rabaud, D. Salin, and P. Watzky
Laboratoire F.A.S.T. (Paris 6 et 11, et CNRS), Bât. 502, Campus Universitaire, F-91405 Orsay Cedex, France

(Received 19 September 1996; accepted for publication 4 February 1997)

The parallel flow of one or two fluids of contrasted viscosities through a rectangular channel of large aspect ratio is studied. The usual result for an infinite aspect ratio is that the velocity profile is parabolic throughout the gap and flat in the other direction. For a finite aspect ratio a deviation from this usual profile is found in boundary layers along the edges of the channel or close to the interface. The extension of these boundary layers is of the order of the small dimension of the channel. In the two-fluid case we find, however, that the velocity profile at the interface is strictly a parabola. The velocity profiles obtained by a 3-D lattice BGK simulation are successfully compared to the analytical results in the one- and two-fluid cases. © *1997 American Institute of Physics.* [S1070-6631(97)01106-9]

Since the pioneering work of Hele-Shaw[1] and the determination of Darcy's law,[2] viscous flows between parallel walls have been intensively studied in the last 20 years.[3] A two-dimensional flow in a Hele-Shaw cell is known to be analogous to the flow in a three-dimensional porous medium. When two fluids of contrasted viscosities flow in the cell, the interface can be unstable, leading to the so-called Saffman–Taylor instability, when the less viscous fluid forces the more viscous one to recede. In the case of a parallel flow, it has been shown that made up solitons can propagate along the interface.[4] We have found experimentally that for large enough flow rates, regular waves propagate along the interface.[5] In this Brief Communication, we address the case of Laminar parallel flow taking into account the finite aspect ratio of the cell and a horizontal interface between the two fluids.

Let us first consider one fluid of dynamic viscosity μ flowing under the pressure gradient G in a rectangular duct of large aspect ratio h/e (Fig. 1). For a stationary parallel flow, the velocity $u(y,z)$ along the flow direction x satisfies Poisson equation, $\nabla^2 u(y,z)=-G/\mu$, with no-slip boundary conditions at the walls $u(\pm e/2,z)=0$ and $u(y,\pm h/2)=0$. When $e<h$, it is convenient to split the velocity field into two terms: $u(y,z)=u^*(y)+u^{**}(y,z)$. The first one, $u^*(y)$, is the velocity in the infinite case (no end walls in z direction); its expression is the well-known parabolic Haagen–Poiseuille profile: $u^*(y)=u_0[1-(2y/e)^2]$ with $u_0=Ge^2/(8\mu)$. The second term, $u^{**}(y,z)$, takes into account the two end walls located at $z=\pm h/2$. It satisfies Laplace equation $\nabla^2 u^{**}(y,z)=0$ with the boundary conditions $u^{**}(\pm e/2,z)=0$ and $u^{**}(y,\pm h/2)=-u_0[1-(2y/e)^2]$. Assuming a Fourier decomposition of $u^{**}(y,z)$ where each term is the product of a y function by a z function, and taking into account the boundary conditions and that $u^{**}(y,z)$ is an even function of y and z, leads to the velocity field $u(y,z)$:

$$u(y,z)=\frac{Ge^2}{8\mu}\left\{1-\left(\frac{2y}{e}\right)^2+\sum_{n=1}^{\infty}(-1)^n\frac{32}{(2n-1)^3\pi^3}\times\frac{\cosh((2n-1)\pi(z/e)}{\cosh((2n-1)\pi/2\ h/e)}\cos\left((2n-1)\pi\frac{y}{e}\right)\right\}. \quad (1)$$

Note that the length scale over which the velocity varies in each direction is the thickness e, the height h being only involved through the aspect ratio h/e. The successive terms of the sum decrease rapidly, roughly as $1/n^3$. Figure 2 shows the velocity as a function of y at different distances from the end walls. The profile in y looks parabolic with a maximum velocity equal to the one in a cell of infinite aspect ratio, provided that the distance from the end walls is larger than the thickness of the cell. The profile departs weakly from quadratic only close to the end walls, the maximum of the profile going to zero as the distance from the end walls goes to zero. The numerical simulations, based on a lattice BGK technique described hereafter, have been performed in a rectangular channel of aspect ratio $h/e=10$ with 20×200 nodes for the channel section. The simulation results are in very good agreement with the analytical curves despite the rather small number of nodes (20) in y direction. Figure 3 shows the velocity as a function of z for different aspect ratios in the $y=0$ plane. Provided that the aspect ratio is larger than two, the profile is clearly nonparabolic but flat except near the walls. The boundary layers diffusion from the end walls is hindered by the other two walls. Hence, their extension is given by the thickness of the cell. The agreement between the analytical curves and the simulation results is again very good.

Let us now consider the parallel flow of two fluids 1 and 2, of dynamic viscosities μ_1 and μ_2 driven by the same pressure gradient G. We restrict ourselves to the case where the interface (at $z=0$) between the two fluids is flat. In laboratory experiments, this condition is achieved when the upper fluid is less dense than the other (the interface is stabilized by gravity and interfacial tension if any), and when the flow rates of the two fluids are sufficiently low. At last this

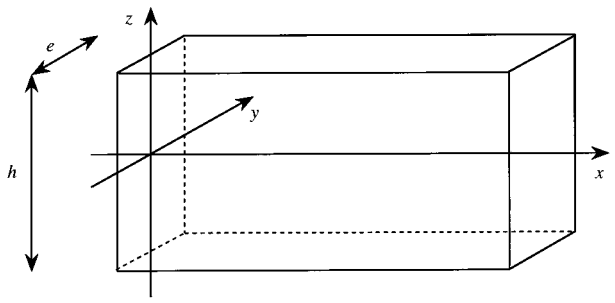

FIG. 1. Geometry of the cell: $-h/2 \leqslant z \leqslant h/2$ and $-e/2 \leqslant y \leqslant e/2$.

assumes a contact angle of $\pi/2$ at the wall which occurs with miscible fluids only. Unlike previous studies,[6] we focus on the velocity profile near the interface in the case where the latter is located at a distance from the end walls large compared to the thickness e of the cell. According to the results obtained above, the presence of the end walls can then be neglected. The velocities of both fluids along x direction, $u_1(y,z)$ for $z \geqslant 0$ and $u_2(y,z)$ for $z \leqslant 0$, satisfy Poisson equation, $\nabla^2 u_i(y,z) = -G/\mu_i$ $(i=1,2)$, with no-slip boundary conditions, $u_i(\pm e/2,z)=0$, continuity of the velocity at the interface, $u_i(y,0)=u_I(y)$, where $u_I(y)$ is the unknown velocity profile at the interface, and continuity of the tangential stresses at the interface, $\mu_1(\partial u_1/\partial z)(y,0)=\mu_2(\partial u_2/\partial z)(y,0)$. We split again the velocity u_i into two terms: $u_i(y,z)=u_i^*(y)+u_i^{**}(y,z)$. The first term $u_i^*(y)=u_{i_0}(1-(2y/e)^2)$ with $u_{i_0}=Ge^2/(8\mu_i)$ is the unperturbed velocity far away from the interface. The second one, $u_i^{**}(y,z)$, satisfies Laplace equation $\nabla^2 u_i^{**}(y,z)=0$ with the boundary conditions $u_i^{**}(\pm e/2,0)=0$, $u_i^{**}(y,0)=u_I(y)-u_{i_0}(1-(2y/e)^2)$ and $\mu_1(\partial u_1^{**}/\partial z)(y,0)=\mu_2(\partial u_2^{**}/\partial z)(y,0)$. Writing $u_i^{**}(y,z)$ as a sum of Fourier terms and taking the boundary conditions into account, we find the velocity profile at the interface:

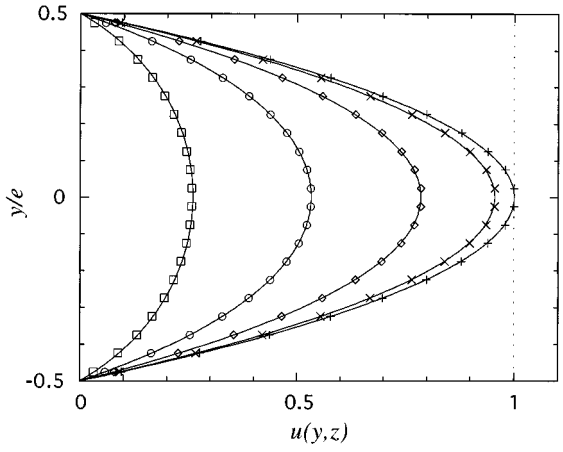

FIG. 2. Velocity profile $u(y,z)$ in the xOy plane for different distances $d=h/2-|z|$ from the end walls in a cell of large aspect ratio. Analytical results (solid lines) and corresponding lattice BGK simulation (symbols) for $d \gg e$ (+), $d=e$ (×), $d=e/2$ (◇), $d=e/4$ (○), and $d=e/10$ (□). The velocity is normalized by the plane Poiseuille flow maximum velocity $Ge^2/(8\mu)$.

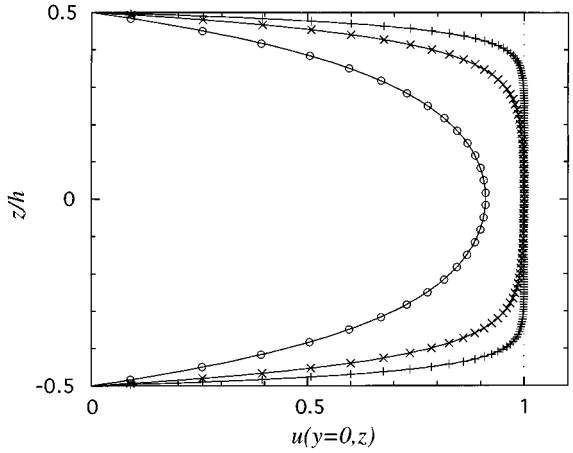

FIG. 3. Normalized velocity profile $u(0,z)$ in the xOz plane for different aspect ratios h/e: analytical results (solid lines) and simulation (symbols) for $h/e=2$ (○), $h/e=5$ (×), and $h/e=10$ (+).

$$u_I(y) = \frac{\mu_1 u_{1_0} + \mu_2 u_{2_0}}{\mu_1 + \mu_2}\left[1 - \left(\frac{2y}{e}\right)^2\right], \tag{2}$$

where we use the relation $\mu_1 u_{1_0} = \mu_2 u_{2_0} = Ge^2/8$. The interface velocity appears as the average, weighted by their viscosities, of the unperturbed velocities of the two fluids. Using the expression of $u_I(y)$ in the equation of continuity for the velocity at the interface, we finally get the velocity profile in each fluid:

$$u_i(y,z) = \frac{Ge^2}{8\mu_i}\left\{1 - \left(\frac{2y}{e}\right)^2 + \varepsilon_i \frac{\mu_1\mu_2}{\mu_1+\mu_2}\sum_{n=1}^{\infty}(-1)^n \times \frac{32}{(2n-1)^3\pi^3}\exp\left(\varepsilon_i(2n-1)\pi\frac{z}{e}\right) \times \cos\left((2n-1)\pi\frac{y}{e}\right)\right\}, \tag{3}$$

with $\varepsilon_i=(-1)^i$ and $i=1,2$. The velocity profiles near the interface are plotted in Fig. 4 for a viscosity ratio $\mu_1/\mu_2 = 0.1$. The extension of the velocity variation scales as the thickness e of the cell in both fluids. When $\mu_1 \ll \mu_2$, the interface velocity is approximately twice that of the more viscous fluid [Eq. (2)]. Again, the simulations give very good results despite the small number of nodes (15) in y direction. We also compare the analytical and the numerical velocity profile at the interface. Note that for the simulation, as there are no nodes on the interface, the interface velocity is obtained by averaging (and weighting by the viscosities) the velocity of each fluid taken on the nodes just above and below the interface. The velocity profile in y is a parabola in each fluid far from the interface, deviates weakly from the parabola near the interface but is again strictly a parabola at the interface. The physical reason for this surprising result is the relation satisfied by the velocity curvatures in z direction at the interface, $(\partial^2 u_i/\partial z^2)(y,0)$. These terms do not depend on y coordinate[7] and they are linked together by $\mu_1(\partial^2 u_1/\partial z^2)(y,0) = -\mu_2(\partial^2 u_2/\partial z^2)(y,0)$. Hence, by adding the two Poisson equations satisfied by the two fluids at

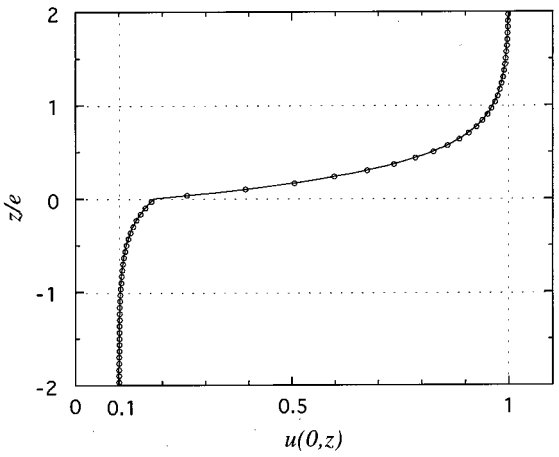

FIG. 4. Velocity profile $u(0,z)$ near the interface between two fluids of viscosity ratio $\mu_1/\mu_2=0.1$ flowing in a cell of large aspect ratio: analytical results (solid line) and simulation (○). The velocity is normalized by the plane Poiseuille flow maximum velocity of the less viscous fluid $Ge^2/(8\mu_1)$.

the interface, the z derivatives compensate each other and we easily obtain $(\mu_1+\mu_2)(\partial^2 u_I/\partial y^2)(y)=-2G$ which leads to the parabola for the interface velocity.[8] Note that this result is no longer true if the interface is close to an end wall.

For the simulations, we use in this work the BGK model with the so-called D3Q19 lattice (for 3 dimensions and 19 lattice directions). Applying the statistical physics ideas of Bhatnagar *et al.*,[11] Qian *et al.*[12] have developed the lattice BGK model to simulate a viscous fluid flow. Following Qian *et al.*, a relaxation equation governing the time evolution of the mass density $N_i(\mathbf{r},t)$ in the direction i, at time $t+1$ is used.[11] The model leads to the Newtonian incompressible Navier–Stokes equation, where the kinematic viscosity ν of the fluid can be easily tuned through one relaxation parameter fixed at the beginning of the simulation.

The simulations are performed on a lattice of size $N_x\times N_y\times N_z$, where $N_x=1$, N_y is equal to 15 or 20, and N_z varies between 30 and 200. Since the flow does not depend on the coordinate x, only one row is needed when periodic boundary conditions are applied in the flow direction; bounce-back boundary conditions are applied on the first and last nodes of the lattice, in y and z directions. The walls are therefore at half a node away from these nodes, giving a cell thickness $e=N_y$ and a cell height $h=N_z$. The algorithms are implemented on CM5 and Cray-T3D computers. Parallelism is definitely suitable for lattice modeling, owing to the independence of each node: collision and propagation steps can be achieved simultaneously for all nodes. Physical variables are related to lattice ones (denoted by L) as follows: $\nu=\nu_L(l^2/t_0)$ and $U=U_L(l/t_0)$, where l is the lattice spacing and t_0 is the time step.

The simulations of one-fluid flow have been performed using a kinematic viscosity $\nu_L=0.01$ and an average fluid velocity $U_L=0.005$ (Figs. 2 and 3). In Fig. 2, a lattice size of $N_y\times N_z=20\times 200$ has been used leading to an aspect ratio $h/e=10$. In Fig. 3, $N_y=15$ and $N_z=30$, 75, and 150, leading to aspect ratios $h/e=2$, 5, and 10, respectively. The Reynolds number $\mathrm{Re}=U_L N_y/\nu_L$ is less than 10 when evaluated with the thickness $N_y=15$. The stationary state flow is achieved after typically 50 000 time steps, which corresponds to the viscous diffusive time on the spatial scale e ($t\approx N_y^2/\nu_L\approx 40\,000$). The typical computing time is 5 CPU minutes for a 32 node-partition of the CM5 computer.

For the two-fluid flow case (Fig. 4) a lattice of size $1\times 15\times 150$ has been used. The fluids of different viscosities, but with the same densities, lie on top of each other (each fluid occupying half of the lattice nodes in z direction). There is no surface tension between the fluids but they are not allowed to mix.[11] The kinematic viscosities are equal to 0.1 and 0.01, yielding to a viscosity ratio of $\mu_1/\mu_2=0.1$, and the Reynolds number is equal to 0.9 when evaluated with the smaller viscosity and the thickness. The flow is thus clearly in the laminar regime.

This description of the stable flow of two superimposed viscous fluids in a Hele-Shaw cell is a first step in the understanding of the shear instability existing in such an experimental setup.[5]

ACKNOWLEDGMENTS

Computer time has been provided by CNCPST and IDRIS. One of us (P.G.) thanks Elisabeth Charlaix for stimulating discussions.

[1] H. J. S. Hele-Shaw, ''On the motion of a viscous fluid between two parallel plates,'' Nature **58**, 34 (1898).
[2] H. Darcy, *Les Fontaines Publiques de la Ville de Dijon: Distribution d'eau et Filtrage des Eaux* (Victor Dalmont, Paris, 1856).
[3] P. Saffman and G. I. Taylor, ''The penetration of a fluid into a porous medium or Hele-Shaw cell containing a more viscous liquid,'' Proc. R. Soc. London **39**, 65 (1958); D. Bensimon, L. P. Kadanoff, S. Liang, B. I. Shraiman, and C. Tang, ''Viscous flows in two dimensions,'' Rev. Mod. Phys. **58**, 977 (1986).
[4] M. Zeybek and Y. C. Yortsos, ''Parallel flow in Hele-Shaw cells,'' J. Fluid Mech. **241**, 421 (1992).
[5] P. Gondret and M. Rabaud, ''Gas-liquid shear instability in a Hele-Shaw cell,'' Communication at the Euromech Colloquium on ''Interfacial Instabilities, 11–13 September 1996, Palaiseau/Paris, France.
[6] Y. P. Tang and D. M. Himmelblau, ''Velocity distribution for isothermal two-phase co-current laminar flow in a horizontal rectangular duct,'' Chem. Eng. Sci. **18**, 143 (1963); A. Nadim, A. Borhan, and H. Haj-Hariri, ''Tangential stress and Marangoni effects at a fluid-fluid interface in a Hele-Shaw cell,'' J. Colloid Interface Sci. **181**, 159 (1996).
[7] Indeed, $-\Sigma_{n=1}^{\infty}(-1)^n[4/(2n-1)\pi]\cos((2n-1)\pi(y/e))$ is equal to 1 in the interval $-e/2\leqslant y\leqslant e/2$.
[8] Note that in Eq. (3) the infinite summation for $z=0$ is the Fourier decomposition of $1-(2y/e)^2$ in the interval $-e/2\leqslant y\leqslant e/2$.
[9] P. L. Bhatnagar, E. P. Gross, and M. Krook, ''A model for collision processes in gases: I. Small amplitude processes in charged and neutral one-component systems,'' Phys. Rev. **94**, 511 (1954).
[10] Y. H. Qian, D. d'Humières, and P. Lallemand, ''Lattice BGK models for Navier–Stokes equation,'' Europhys. Lett. **17**, 479 (1992).
[11] N. Rakotomalala, D. Salin, and P. Watzky, ''Simulations of viscous flows of complex fluids with a Bhatnagar–Gross–Krook lattice gas,'' Phys. Fluids **8**, 3200 (1996).